JOURNAL OF THERMOPHYSICS AND HEAT TRANSFER
Vol. 12, No. 4, October–December 1998

Nonequilibrium Vibrational Distributions of N_2 in Radio-Frequency Parallel-Plate Reactors

S. Longo* and M. Capitelli†
University of Bari, 70126 Bari, Italy
and
K. Hassouni‡
Université de Paris Nord, 93430 Villetaneuse, France

A self-consistent code has been realized to describe and simultaneously interrelate the nonequilibrium molecular vibrational kinetics and the plasma dynamics in a parallel-plate radio frequency discharge in pure nitrogen. The code is based on a one-dimensional in space and two-dimensional in space velocity, particle-in-cell with Monte Carlo collisions model of the plasma dynamics coupled to a set of one-dimensional diffusion-reaction equations for the population of vibrational states of nitrogen molecules in the electronic ground state $N_2(X, v)$ and for the density of nitrogen atoms, with appropriate catalytic boundary conditions. The code gives information about the plasma dynamics (electron and ion density, mean energy, drift velocity, electric field in the discharge, etc.), the vibrational distribution function, the electron energy distribution function, and the atomic concentration in the discharge. It is shown that a self-consistent approach is essential to accurately calculate the discharge properties.

Nomenclature

D_i = diffusion coefficient of the ith species, $m^2\ s^{-1}$
e = electron charge, C
f = frequency, s^{-1}
$f(\varepsilon)$ = electron energy distribution function, $eV^{-3/2}$
k = Boltzmann's constant, $eV\ k^{-1}$
l = discharge gap, m
m_e = electron mass, kg
m_i = mass of the ith species, kg
n_i = number density of the ith species in the plasma, m^{-3}
p_{Nv} = $N_2(X, v)$ yield from surface N–N recombination
p_{wv} = $N_2(X, v)$ yield from surface $N_2(w)$ deactivation
q = conversion factor, 1.6×10^{-19} J eV^{-1}
R_i^p, W_i^+ = contribution to the rate of formation of the ith species caused by the process p, units depend on reaction order
T_{01} = vibrational temperature defined according to the population of $N_2(v = 0)$ and $N_2(v = 1)$, K
V_{rf} = amplitude of the oscillating radio frequency voltage, V
v = vibrational quantum number
v_i^{th} = thermal speed of the ith neutral species in the plasma, $m\ s^{-1}$
x = position, m
γ_s = loss probability at the wall for the species s
ΔW_i^- = linearized contribution to the rate of destruction of the ith, units depend on reaction order
$\Delta\varepsilon_{01}$ = energy threshold for $v = 0 \rightarrow v = 1$ vibrational excitation, eV
ε = electron energy, eV
$\sigma_p(\varepsilon)$ = cross section for the electron–molecule elementary process p as a function of the electron energy, m^2

Presented as Paper 97-2363 at the AIAA 28th Plasmadynamics and Lasers Conference, Atlanta, GA, June 23–25, 1997; received Sept. 13, 1997; revision received Feb. 20, 1998; accepted for publication March 4, 1998.

*Researcher, Chemistry Department, Centro di Studio per la Chimica dei Plasmi del CNR, Via Orabona 4.
†Professor, Chemistry Department, Centro di Studio per la Chimica dei Plasmi del CNR, Via Orabona 4.
‡Researcher, CNRS Villetaneuse.

I. Introduction

In many plasma systems of technological interest (electric discharge reactors for material processing, gas lasers, etc.), high-temperature electrons (some 10^4 K) exist in small concentrations in a bath of cold bulk gas (from room temperature to 10^3 K). In such a nonequilibrium media (cold plasmas) the population distribution of the electronic and vibrational states of molecules and the electronic states of atoms are unable to be portrayed by a Boltzmann law, and the translational energy distribution of the charged particles is not described by a Maxwell–Boltzmann law.[1] While comprehensive calculations of such distribution functions were performed for uniform plasmas,[2] many questions remain regarding the uniformity of the gases and plasmas. Attempts have been made in the framework of local approximations only, i.e., to solve the Boltzmann equation for a locally uniform discharge in the presence of a weak electric field.[3] The local approximation, however, cannot be applied to low-pressure gas discharges and to many other important systems.

In a previous work, the coupling of plasma dynamics and neutral reaction/diffusion models was considered, based on a one-dimensional particle-in-cell with Monte Carlo collisions (PIC–MCC) model for the plasma dynamics.[4] The PIC–MCC model was coupled to a simplified vibrational kinetics describing the low vibrational levels of N_2 under the action of the eV processes (electron impact vibrational excitation and deexcitation of molecules) and the deactivation of vibrationally excited molecules on the wall. The wall phenomenon was described by introducing appropriate boundary conditions for the chemistry-transport code. The model allowed us to study the mutual effect of superelastic vibrational collisions on the electron energy distribution function (eedf) and on the vibrational distribution function (vdf) as well as the effect on the eedf of the deactivation rate of vibrationally excited molecules on the surface wall.

Such a model completely disregarded the presence of vibrational levels with $v > 8$ as well as vibration–vibration (VV)

and vibration–translation (*VT*) energy transfer processes and dissociation–recombination kinetics. In this work, we present an extended version of the method that takes into account the entire vibrational ladder of the electronic ground state of nitrogen molecules $N_2(X, v)$ as well as the presence of the nitrogen atoms. Moreover, we consider both a ladder-climbing mechanism for the dissociation of N_2 as well as the direct dissociation by electron impact. This leads to a system of 47 coupled nonlinear equations for reaction and diffusion (one each for all vibrational levels plus one for N atoms). Because the rate coefficients for electron–molecule reactions depend on the eedf, the system must be solved consistently with the results of the particle code, which is in turn affected by the state-to-state kinetics.

II. PIC–MCC Modeling of Electron and Ion Dynamics

The PIC–MCC method has been described elsewhere.[5] Briefly, it consists of a particle simulation of both electron and ion dynamics, including space charge effects and electron and ion collisions with neutrals. The space charge field is calculated by solving the Poisson equation on an appropriate mesh, whereas collisons with neutrals are included by using a Monte Carlo method. Our version of the model[4] is one-dimensional in space but two-dimensional in space velocity.[4] Two dimensions are sufficient here because of the axial symmetry and the absence of a magnetic field. Particle positions and velocities are updated at every time step using the leap-frog method. This information is fed to the calculation of the charge density in the one-dimensional Poisson equation following the first-order [cloud in cell (CIC)] sampling rule.[5] The same rule is used to interpolate the electric field acting on each particle from the values calculated at each grid point. The particle ensemble is reduced to one-half in case the particle number becomes excessively high, and the simulated particle weight is modified accordingly; the opposite procedure is taken if the particle number becomes too low.

The boundary conditions are derived from the value of the electric potential at the two boundary surfaces $x = 0$ and $x = 1$, and the absorption probability for electrons and ions by the surfaces and the probability of electron emission by the surface caused by ion impact. In the calculations presented in this paper, we assumed that electrode surfaces are completely absorbing for both electrons and ions, and the probability of ion-collision electron emission is set to zero. Electron-neutral[6] and ion-neutral collision processes are introduced according to the appropriate cross sections using the null-collision, test-particle Monte Carlo method.

The approach used here is that of storing a separate time-to-next-collision for any particle, and the allowance of a possible collision at any time of the simulation (not necessarily at the end of the leap-frog time step). This approach is somewhat computationally expensive but it can be used for fairly high gas pressures. For the specific system under examination, only electrons and N_2^+ ions are moved as particles. The following collision processes are considered: Elastic collisions of electrons with N_2 molcules; inelastic processes leading to rotational, vibrational, and electronic excitation of N_2 molecules; electron impact ionization of N_2; and elastic and charge-exchange collisions of N_2^+ ion with N_2. Electron–atom processes have been neglected because of their small concentration of atoms (see the Results section).

Two different ion-neutral processes are considered: Elastic collisions and charge exchange. For both processes the collision frequency is calculated from the known cross sections. Elastic scattering is treated as a rigid-sphere isotropic scattering, assuming that the neutrals move at thermal speed in random directions. Charge exchange is treated by assigning the thermal speed to the impinging ion in random directions. The cross sections used are extracted from Ref. 7. The original feature of our PIC–MCC code is the self-consistent coupling with the state-to-state chemical kinetics. The coupling between PIC–MCC and vibrational kinetics occurs through collisions of the second kind (exothermic). The eedf depends on the concentration of vibrationally excited states and, therefore, on the vibrational kinetics that in turn depend on eedf through *eV* rates.

III. Nonequilibrium Vibrational and Dissociation Kinetics

The coupled chemical kinetics and transport in the N_2 plasma was investigated by considering 46 vibrational levels of N_2 molecules as well as N atoms. The electron impact vibrational excitation processes that have been taken into account are

$$N_2(v) + e \rightarrow N_2(v + i) + e, \qquad i = 1\text{–}8 \tag{1}$$

i.e., vibrational inelastic collisions, and

$$N_2(v + i) + e \rightarrow N_2(v) + e, \qquad i = 1\text{–}8 \tag{2}$$

i.e., vibrational superelastic or second-kind collisions. In addition to the electron impact processes, we have also considered the *VV* and *VT* relaxation kinetics that involve the following processes:

$$\begin{gathered} N_2(v) + N_2(w) \rightarrow N_2(v - 1) + N_2(w + 1) \\ N_2(v) + N_2 \quad \text{or} \quad N \rightarrow N_2(v - 1) + N_2 \quad \text{or} \quad N \end{gathered} \tag{3}$$

The reactions rate constants of these processes were estimated from the Schwertz-Slovesky-Herzfeld (SSH) theory. The N_2 dissociation by the *VV* pumping channel has been taken into account by considering an extra pseudolevel $N_2(v = 46)$ and the following *VV* and *VT* dissociative collisions:

$$\begin{gathered} N_2(v) + N_2(45) \rightarrow N_2(v - 1) + 2N \\ N_2(45) + N_2 \quad \text{or} \quad N \rightarrow 2N + N_2 \text{ or } N \end{gathered} \tag{4}$$

The rate constants of the preceding processes have been also estimated by scaling the value for the $0, 1 \rightarrow 1, 0$ transition obtained in Ref. 8 with the SSH theory. The present model includes direct dissociation of $N_2(v = 0)$ by electron impact, for which we used the cross section reported in Ref. 9.

The transport of the different vibration levels of N_2 and N atoms in the investigated discharge is purely diffusive. Therefore, the transport of each species is governed by the balance between the diffusive fluxes and the chemical source term. Because the gas temperature is assumed to be constant over the entire discharge field, the set of coupled nonlinear diffusion equations governing the plasma species transport can be written as

$$\begin{gathered} D_v \frac{\partial^2 n_v(x)}{\partial x^2} + R_v^{eV} + R_v^{VV} + R_v^{VT} = 0 \\ D_N \frac{\partial^2 n_N(x)}{\partial x^2} + R_N^{dd} + R_N^{lc} + R_N^{br} = 0 \end{gathered} \tag{5}$$

where the different chemical source terms correspond to the *eV* processes, *VV* and *VT* relaxation processes, direct dissociation (dd), ladder-climbing dissociation (lc), and recombination in the bulk plasma (br). The subscript represents a plasma species [$N_2(v = 0\text{–}45)$ or N], n and D are the particle number density and diffusion coefficient of a given species, and x denotes the axial coordinate of the discharge. The explicit expressions for the contribution of an *eV* process such as

$$N_2(v') + e \rightarrow N_2(v) + e \tag{6}$$

to the source term $R^{eV}_{v'\to v}$ is

$$R^{eV}_{v'\to v} = n_e n_{v'} \left(\frac{2q}{m_e}\right)^{1/2} \int_0^\infty d\varepsilon \sigma_{v'\to v}(\varepsilon)\varepsilon f(\varepsilon) \tag{7}$$

where n_e is the electron number density, $\sigma(\varepsilon)$ is the process cross section, and $f(\varepsilon)$ is the eedf normalized to satisfy the following condition:

$$\int_0^\infty d\varepsilon \varepsilon^{1/2} f(\varepsilon) = 1 \tag{8}$$

The source term thereby depend on the entire shape of $f(\varepsilon)$ and not only on the electron temperature. The time-averaged eedf is calculated as a function of position and energy, and the electron number density is calculated as a function of position by the PIC–MCC part of the code. For the cross sections, we extrapolated the available data[6] by using the scaling relation

$$\begin{aligned} \sigma_{v\to v+k}(\varepsilon) &= \sigma_{0\to k}(\varepsilon - \Delta\varepsilon_{vk}) \\ \Delta\varepsilon_{vk} &= (\varepsilon_k - \varepsilon_0) - (\varepsilon_{v+k} - \varepsilon_v) \end{aligned} \tag{9}$$

where ε_i denotes the vibrational energy of level $N_2(i)$. This scaling relation assumes that vibrational excitation processes are the same as long as the energy difference between the initial and the final states are the same and the cross sections have the same shapes and maximum values. The only difference between cross sections concerns the energy threshold that varies according to the anharmonicity of the N_2 molecule.

The cross sections of the superelastic processes have been estimated from those of the inelastic ones from the detailed balance principle.

The role of surface must be considered either for the deactivation of vibrationally excited molecules or for the recombination of atomic nitrogen. Accordingly, we introduced the following catalytic boundary conditions for the electrode surfaces (dissociation of vibrationally excited molecules on the surface is neglected):

$$\begin{aligned} \left.\frac{\partial n_v(x)}{\partial x}\right|_{x=0} &= -\frac{R_v}{4D_v} \\ \left.\frac{\partial n_N(x)}{\partial x}\right|_{x=0} &= -\frac{R_N}{4D_N} \\ R_N &= -v_N^{th}\gamma_N n_N(0) \\ R_v &= -v_v^{th}\gamma_v n_v(0) + \sum_w p_{wv} v_w^{th}\gamma_w n_w(0) + \frac{1}{2} p_{Nv} v_N^{th}\gamma_N n_N(0) \end{aligned} \tag{10}$$

where R_s is the rate of production of the species s because of surface reactions. Analogous equations fix the boundary conditions at $x = 1$ (right electrode). In the following calculations we assumed for simplicity that all molecules deactivate to $v = 0$, and atom recombination results in an N_2 molecule in the vibrational level $v = 0$. The set of Eqs. (3) and (4) has been discretized on a one-dimensional grid using a central finite difference scheme. Because the chemical source terms of the different species present a very strong stiffness, they were split in two parts and linearized according to

$$W_s = W_s^+ - \Delta W_s^- n_s \tag{11}$$

where W_s^+ and $\Delta W_s^- n_s$ represent the production and consumption rates of species s. This numerical treatment results in a set of nonlinear algebraic equations solved using a Gauss–Siedel line relaxation technique.

IV. System Under Examination and Calculation Conditions

The model was applied to a discharge in pure nitrogen, produced in a parallel-plate, high-frequency reactor with the two plates separated by 4 cm. The pressure assumed in our study is $p = 0.1$ torr (at $T = 300$ K). One of the plates (the so-called *grounded electrode*) is constantly kept at zero voltage, whereas the other (the powered electrode) is driven by an external generator to an oscillating voltage $V(t) = V_{rf} \sin 2\pi ft$. Calculated results depend on the applied voltage V_{rf}, on the rf frequency f as well on the pressure. The deactivation probability of vibrationally excited N_2 molecules on limiting surfaces and the recombination of atomic nitrogen on the surfaces can be treated as parameters as well. In our calculations we assumed $V_{rf} = 200$ and 500 V, whereas f was set equal to 13.56 MHz. The number of simulated particles in these PIC–MCC calculations was between 10,000 and 20,000, the number of mesh cells was equal to 400, and the time step considered was equal to 10^{-10} s. These values assure the stability of the code for thermal electron motion, electron plasma oscillations, and Debye screening.[5] To ensure convergence the simulated time was 3×10^{-4} s, about 4000 rf cycles. For the chemical kinetics we set $\Delta x/l = 1/40$ and fixed the value of deactivation probability on the surface to 10^{-3} (a realistic value for metal surfaces), whereas different values were selected for the atom recombination probability. Where not differently specified, calculations were performed assuming a recombination probability of 10^{-1}. This last parameter, however, has little effect on the electrical characteristics of the discharge.

V. Results

In Fig. 1 the time-averaged concentration of electrons and ions in the discharge are presented as a function of position in the steady state. One can observe here the classical parallel-plate limited electron dynamics, with reduced ionization degree in the sheath (plasma boundary) region. In an rf discharge the edge of both sheaths performs an oscillatory motion at the rf frequency, and so it accelerates toward the bulk plasma the electrons that found themselves inside an expanding sheath region. This plasma dynamics can be better appreciated by looking at Figs. 2 and 3, showing respectively, the charged particle mean energy and drift velocity. As can be seen, the electron mean energy is quite high at the edge of the sheath region, and decreases in the bulk, where it is, however, still far higher than the ion mean energy. The ions in the bulk plasma are at room temperature because of the effective energy exchange with the neutral particles, but they gain energy when entering the sheath region, where they are progressively accelerated toward the electrode surfaces. As can be seen, the electron and ion drift velocities in the bulk plasma have the same sign, thereby illustrating the nonlocal conditions of calculations and the regime of ambipolar diffusion. The fluxes of electrons and ions to the electrodes are in fact the same, and the drift velocity ratio balances the lower electron density in the sheath region.

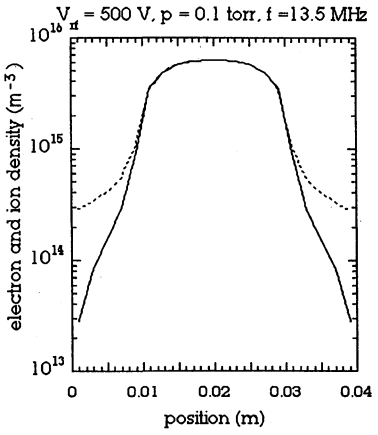

Fig. 1 Steady-state, time-averaged electron (——) and N_2^+ ion (---) density.

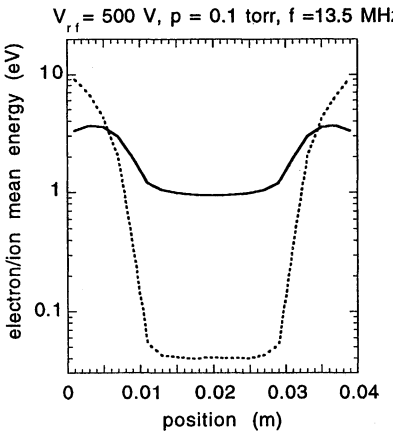

Fig. 2 Steady-state, time-averaged electron (——) and N_2^+ ion (---) mean energy.

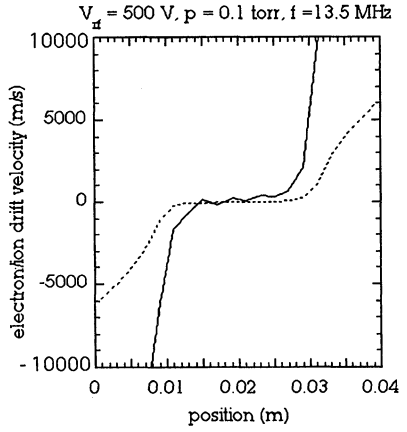

Fig. 3 Steady-state, time-averaged electron (——) and N_2^+ ion (---) drift velocity.

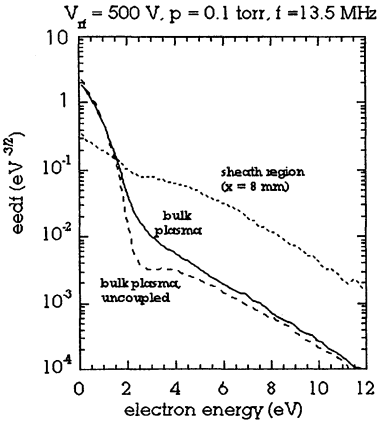

Fig. 4 Steady-state, time-averaged electron energy distribution function.

Figure 4 shows the eedf for two different positions in the discharge gap: In the bulk plasma and in the sheath region. As can be seen here, the high electron temperature in the sheath region is reflected in the bulk plasma, which is characterized by a low-energy region that represents most of the electrons, and the long tail as a result of the diffusion of fast electrons from the sheath region. The shape of this eedf is very different from the Maxwell–Boltzmann shape (this shows itself as a straight line in the plot of Fig. 4). It is important to observe the strong difference in the energy region 2–4 eV between the bulk plasma eedf calculated with the full code and the eedf calculated by using the PIC–MCC code only. The difference between the two eedfs is because of the presence of superelastic electron collisons with vibrationally excited nitrogen molecules in the full code. In Fig. 5, the calculated vdf in the plasma is shown. Because of the low value of g_v, the vdf is practically independent on position and its shape is mainly determined by bulk plasma relaxation phenomena. It can be observed that the vdf also depends on the value of V_{rf}. The calculated vdfs have a non-Boltzmann shape and can be characterized by three regions: 1) The low temperature, low v region; 2) the region of medium v and high vibrational temperature caused by the fast VV processes; and 3) the tail, where the vibrational temperature is lower because of the VT processes, which are effective for high v. A T_{01} temperature can be defined as

$$T_{01} = \frac{\Delta\varepsilon_{01}}{k}\left(\ell n \frac{n_0}{n_1}\right)^{-1} \tag{12}$$

where $\Delta\varepsilon_{01}$ is the $(v = 0) \rightarrow (v = 1)$ energy threshold. The value of T_{01} is presented in Fig. 6. It can be seen that T_{01} is a very weak function of the position but that it strongly depends on the value of V_{rf}. It is important to underline that to obtain these results one must self-consistently couple the plasma dynamics and the electron kinetics, as observed for the eedf. In fact, if one solves the kinetic problem using the electron–molecule source terms obtained by a simple PIC–MCC calculation, the difference between the two eedfs observed in Fig. 4 results in a lower eV source terms and, consequently, the T_{01} vibrational temperature is also lower. In particular, the result at V_{rf} = 500 V for T_{01} obtained by decoupling the PIC–MCC

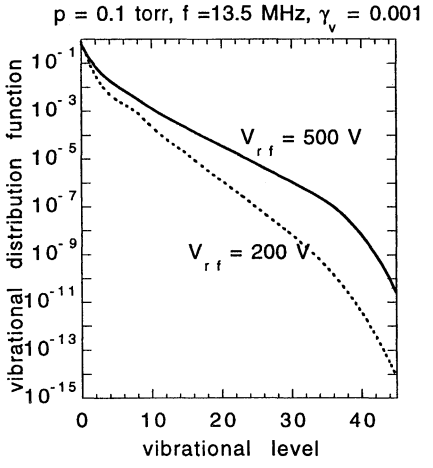

Fig. 5 Vibrational distribution function.

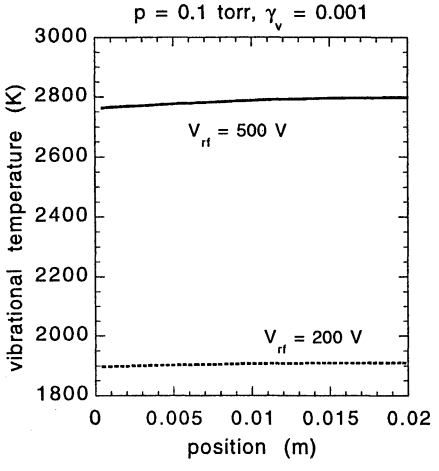

Fig. 6 T_{01} vibrational temperature.

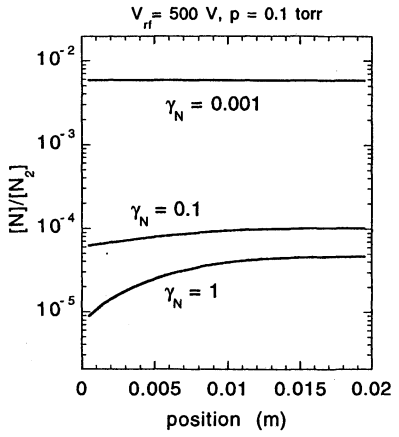

Fig. 7 Mole fraction of the N atoms calculated for different values of γN.

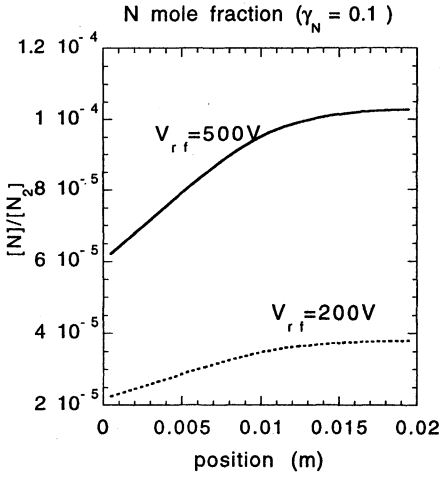

Fig. 8 Mole fraction of the N atoms calculated for different values of V_{rf} and for $\gamma N = 0.1$.

and the vibrational kinetics (about 2200 K) is lower by about 20% than the one obtained with the full code.

Let us now discuss the results for dissociation-recombination kinetics. In Fig. 7 the calculated concentration of N atoms in the discharge gap is presented for different values of recombination probability on the surface γ_N. As can be expected, at higher values of γ_N the atom concentration profile is strongly influenced by the boundary condition. The average values of the N atom concentration found here are compatible with the view that they are produced mainly by dissociation through the direct electron impacts. The atom fraction also strongly changes with the applied rf voltage, as a consequence of higher electron impact dissociation rates, as shown in Fig. 8.

VI. Conclusions

Our results indicate the good possibility of realizing a completely self-consistent gas discharge model. The direct comparison with results obtained by simpler methods also shows the importance of the self-consistent approach to accurately calculate both the electron energy distribution function in the bulk plasma and the vibrational temperature. Further work is now in progress to include the role of electronically excited states of nitrogen molecules. It should be noted that we are still considering a very simplified vibrational kinetics. As an example we do not consider the conversion of vibrationally excited molecules into electronically excited ones and vice versa, and we consider electrons as the only responsible of ionization and of electronic excitation processes. Such a simplified kinetics, however, allows us to better understand the complex nonequilibrium kinetics of this plasma. The extension of these results to chemically reactive gas mixtures (for plasma processing purposes and lasers) could be also investigated in the future.

Acknowledgment

This paper was partially supported by the Progetto Strategico Applicazioni Industriali dei Plasmi of the CNR.

References

[1]Capitelli, M. (ed.), "Nonequilibrium Vibrational Kinetics," *Topics in Current Physics*, Vol. 39, Springer–Verlag, Berlin, 1986.

[2]Gorse, C., "Nonequilibrium Plasma Modeling," *Proceedings of the 21st International Conference on Phenomena in Ionized Gases*, Vol. III, APP, Bochum, Germany, 1993, pp. 141–148.

[3]Colonna, G., and Capitelli, M., "Electron and Vibrational Kinetics in Boundary Layer of Hypersonic Flow," *Journal of Thermophysics and Heat Transfer*, Vol. 10, No. 3, 1996, pp. 406–412.

[4]Longo, S., Hassouni, K., Iasillo, D., and Capitelli, M., "Coupled Electron and Molecular Vibrational Kinetics in a 1D Particle-in-Cell Model of a Low Pressure, High Frequency Electric Discharge in Nitrogen," *Journal de Physique*, Vol. 7, No. 3, 1997, pp. 707–718.

[5]Birdsall, C. K., "Particle in Cell Charged Particle Simulation, Plus Monte Carlo Collisions with Neutral Atoms, PIC-MCC," *IEEE Transactions on Plasma Science*, Vol. 19, No. 2, 1991, pp. 68–85.

[6]Phelps, A. V., and Pitchford, L. C., "Anisotropic Scattering of Electrons by N_2 and Its Effect on Electron Transport: Tabulation of Cross Sections and Results," Joint Information Laboratory Astrophysics Information Center Rept. 26, Univ. of Colorado, Boulder, CO, 1985.

[7]Phelps, A. V., "Cross Sections and Swarm Coefficients for Nitrogen Ions and Neutrals in N_2 and Argon Ions and Neutrals in Ar for Energies from 0.1 eV to 10 keV," *Journal of Physical and Chemical Reference Data*, Vol. 20, No. 3, 1991, p. 557.

[8]Billing, G. D., "Nonequilibrium Vibrational Kinetics," *Topics in Current Physics*, Vol. 39, Springer–Verlag, 1986, pp. 85–112.

[9]Winters, H. F., "Ionic Adsorption and Dissociation Cross Section for Nitrogen," *Journal of Chemical Physics*, Vol. 44, No. 4, 1966, pp. 1472–1476.